Available online at www.sciencedirect.com

ScienceDirect

Ceramics International 40 (2014) 2331–2336

CERAMICS INTERNATIONAL

www.elsevier.com/locate/ceramint

Morphology and magnetic properties of barium hexaferrite ceramics synthesized in x wt% NaCl-(100 − x) wt% KCL molten salts

Eda Aydogan, Seray Kaya, Arcan F. Dericioglu*

Middle East Technical University, Department of Metallurgical and Materials Engineering, Ankara 06800, Turkey

Received 15 May 2013; received in revised form 31 July 2013; accepted 1 August 2013
Available online 9 August 2013

Abstract

Micron size barium hexaferrite ($BaFe_{12}O_{19}$) platelets were prepared by the molten-salt synthesis method in various weight proportions of NaCl–KCl salt mixtures as a liquid medium. The effect of molten salt composition—x wt% NaCl and (100 − x) wt% KCl—on the amount of barium hexaferrite phase formation, as well as, on the morphology and magnetic properties of the final products are discussed. Inductively coupled plasma-mass spectroscopy (ICP-MS) was used to determine the solubility of the starting materials in the salts in order to understand the formation mechanism of barium hexaferrite. X-ray diffraction analysis (XRD), scanning electron microscopy (SEM) and vibrating sample magnetometer (VSM) were used to identify the characteristics of the synthesized barium hexaferrite platelets. ICP-MS analysis showed that the Fe_2O_3 solubility is negligible, however, $BaCO_3$ has very high solubility in both molten KCl and NaCl. Quantitative XRD and SEM results showed that molten salt containing 100 wt% NaCl at 900 °C (for 2 h) resulted in the highest production of barium hexaferrite. Further, SEM results showed that KCl-rich molten salt led to the formation of sharper faceted platelet morphology, whereas NaCl-rich ones resulted in more round platelets.

Data from magnetic measurements showed that as the content of NaCl in the molten salt increases, hysteresis losses became higher. This is a characteristic of the achievement of a harder magnetite behavior in the synthesized barium hexaferrite ceramics. The composition of the KCl/NaCl molten salts was shown to play an important role on the extent of barium hexaferrite formation, resulting platelet morphology and the magnetic properties.

Keywords: A. Molten salt synthesis (MSS); B. Morphology; B. Platelets; C. Magnetic properties; D. Ferrites

1. Introduction

Ferrites having certain magnetic and dielectric properties have been used extensively for various purposes, such as permanent magnets, chip inductors [1,2], microwave absorbers, etc. Polycrystalline barium hexaferrite ($BaFe_{12}O_{19}$) is a hexagonal ferrimagnetic ceramic commonly used in permanent magnets [3]. It has a large saturation magnetization, high Curie temperature, excellent chemical stability, high corrosion resistance, and it is easily processed [4].

Various chemical methods such as the sol–gel process [5], hydrothermal synthesis [6], chemical co-precipitation [7], crystallization from a glass precursor [7], spray-pyrolysis [8], and the molten salt method [9] have been used for the production of platelet shaped barium hexaferrite. These methods result in varying particle sizes, morphologies and magnetic properties. The composition and morphology of the resulting ferrite has been reported by Singhal et.al. [8]. It was shown that magnetic properties of the ferrite ceramics are related to the anisotropy of the shape of the particles.

Molten salt synthesis (MSS) is a technique by which large (up to millimeter-size) seed crystals are used in textured barium hexaferrite processing. Such method allows for low temperature synthesis starting from mixed oxides [10]. Reactions can be

*Corresponding author. Tel.: +90 312 2105941; fax: +90 312 2102518.
E-mail addresses: arcan@metu.edu.tr, arcan_dericioglu@yahoo.com (A.F. Dericioglu).

0272-8842/$ - see front matter © 2013 Elsevier Ltd and Techna Group S.r.l. All rights reserved.
http://dx.doi.org/10.1016/j.ceramint.2013.08.002

completed in a relatively short time interval because of the short diffusion distances and high mobility of raw materials in molten salts, in addition to the high reactivity of the salts [11]. Synthesis of barium hexaferrite in NaCl/KCl molten salt solutions from ferric chloride and barium chloride at a single temperature has been studied by Wang et.al. [12]. However, the effect of synthesis temperature and time on the morphology of the barium hexaferrite ceramics has not been reported [12].

In a more recent study performed by Dursun et al. [13], the effect of crystallinity and particle morphology on the magnetic properties was investigated on barium hexaferrite powders. Powders were synthesized using a solid-state calcination and molten salt synthesis methods with KCl as the flux medium.

In the present study, barium hexaferrite platelets with micron sizes were synthesized by molten salt synthesis method using barium carbonate and iron(III) oxide as the raw materials. This specific synthesis method was shown to allow for the preparation of complex oxide ceramics with anisometric morphologies [14,15] which will further facilitate fabrication of bulk materials with crystallographically textured microstructures [16–18]. The effect of synthesis time and temperature, as well as, flux type and concentration on the formation, morphology and the magnetic behavior of barium hexaferrite have been investigated.

2. Materials and methods

In this process, reagent grade powders of Fe_2O_3 (Sigma-Aldrich, 99.999%), $BaCO_3$ (Sigma-Aldrich, 99%), KCl (Sigma-Aldrich, 99%) and NaCl (Sigma-Aldrich, 99.5%) were used as the raw materials. Fe_2O_3 and $BaCO_3$ were mixed in a molar ratio of $Fe_2O_3/BaCO_3$=5.3 [16,19]. In order to determine the mechanism of barium hexaferrite formation in molten salts (either NaCl or KCl), the salt and previously described mixtures were placed in alumina crucibles with 1:1 wt% and heated to 900 °C in air. The oxide/carbonate components were then mixed in a mortar and pestle for 15 min and a typical batch of 0.4 g mixture was calcined at 900 °C for 10 min in 0.4 g NaCl or KCl fluxes.

After each calcination step the mixture was cooled in air and washed with 100 ml of deionized water. The aqueous suspension was filtered and the solution was analyzed using inductively coupled plasma mass spectroscopy (ICP-MS, Perkin-Elmer DRC II, Massachusetts-USA).

To investigate the effects of time and temperature, as well as, flux type on the formation and morphology of barium hexaferrite ceramics, $Fe_2O_3/BaCO_3$ mixtures were added to the salt mixture with the following compositions; 100 wt% NaCl, 90 wt% NaCl–10 wt% KCl, 80 wt% NaCl–20 wt% KCl, 70 wt% NaCl–30 wt% KCl, 44 wt% NaCl–56 wt% KCl (1:1 mol), 70 wt% KCl–30 wt% NaCl, 80 wt% KCl–20 wt% NaCl, 90 wt% KCl–10 wt% NaCl and 100 wt% KCl. The initial mixtures comprised of 50 wt% flux and 50 wt% oxide/carbonate mixture (Fe_2O_3:$BaCO_3$, 5.3:1 mol) were calcined at 850 °C, 900 °C and 950 °C for 1, 2, 2.5 and 3.5 h.

The filtration procedure mentioned above was conducted on all of the calcined, cooled (solidified) and deionized water dissolved mixtures. Quantitative XRD analyses were applied to the solid residues obtained from the flux compositions of 100 wt% KCl, 10 wt% NaCl, 44 wt% NaCl, 90 wt% NaCl and 100 wt% NaCl by using the software of Rigaku D/MAX2200/PC. Rietveld refinement was applied to the XRD analyses using General Structure Analysis System (GSAS) which is based on the non-linear least squares approach. Before starting the GSAS refinement, Configuration Management Process (CMPR) software was utilized to convert the raw data to the GSAS format. The resulting data was then run through GSAS and after several cycles of refinement, structures for all compositions investigated were obtained.

Additionally, the average platelet radius was measured by applying quantitative metallographic analysis on the scanning electron microscope (FE-SEM, FEI 430 NanoSEM, Oregon-USA) images of the solid residues. Magnetic behavior of the synthesized barium hexaferrite ceramics was investigated via magnetic hysteresis curves recorded by vibrating sample magnetometer (VSM) (Cryogenic Limited PPMS, London-UK) at 300 K.

3. Results and discussion

The ICP-MS results used for the investigation of barium hexaferrite formation mechanism in the molten salts showed that the solubility of Fe_2O_3 is near zero in both NaCl and KCl fluxes, while $BaCO_3$ has extensive solubility in both, even after 10 min of calcination (see Table 1). It can be concluded that $BaCO_3$ dissolves in the fluxes and reacts with Fe_2O_3 particles. It is clear from the Table 1 that the solution of the calcined material in deionized water contains either of the corresponding salt cations along with Ba; however, Fe was not detected in either of the solutions.

The platelets were synthesized in order to be used in a further study for the fabrication of textured bulk barium hexaferrite ceramics by utilizing a tape casting technique. Thus, the largest possible platelet radius with high aspect ratio is desired. Calcination time, temperature and flux type were investigated systematically in order to determine the optimum condition to achieve maximum possible platelet size.

Fig. 1 shows the platelet size distribution as a function of flux composition for varying calcination durations and temperatures. In Fig. 1, it is observed that under all conditions platelet size in KCl flux is the smallest. With the increase in the NaCl flux content, platelet size increased. However, after a certain concentration approaching the equi-molar flux composition, platelet size

Table 1
Inductivelycoupled plasma-mass spectroscopy results of mixtures dissolved in deionized water after calcination at 900 °C for 10 min in KCl and NaCl fluxes.

Flux type	Element	Amount (mg/l)
KCl	**Ba**	128 ± 1.0
	K	53 ± 1.0
	Fe	0
NaCl	**Ba**	117.9 ± 1.0
	Na	39.9 ± 0.6
	Fe	0

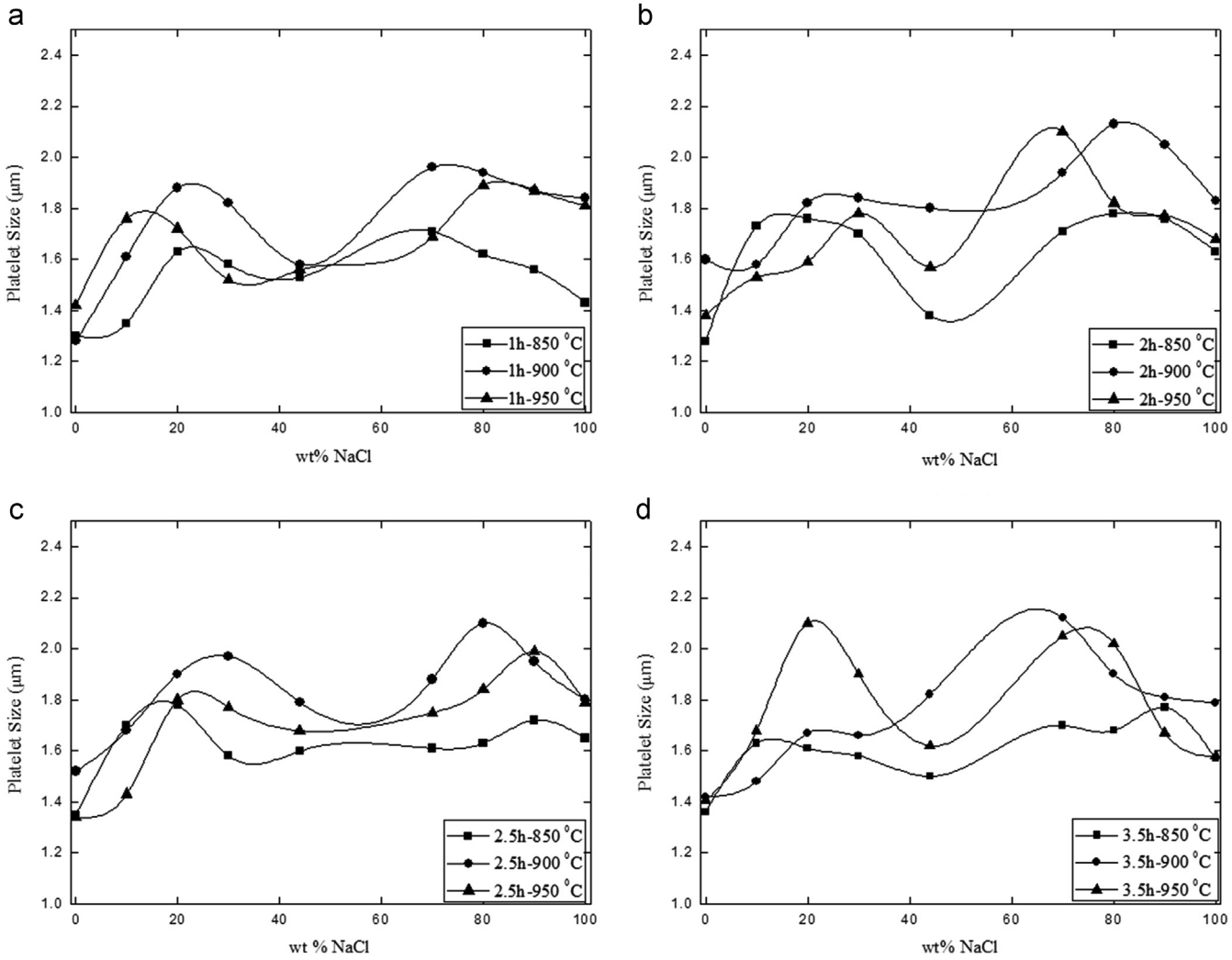

Fig. 1. Particle size as a function of flux composition at 850 °C, 900 °C and 950 °C for (a) 1 h, (b) 2 h, (c) 2.5 h and (d) 3.5 h of calcination.

began to decrease. It should be noted that platelet size in NaCl flux was larger than that in KCl for all the calcination temperatures and durations applied. This demonstrates the lower apparent activation energy for platelet growth in NaCl rich fluxes. As a result, for the same calcination temperatures and durations, the apparent activation energy for platelet growth in NaCl flux should be lower than that in the KCl flux. Compared to other temperatures, platelet size at 900 °C was the largest for most of the compositions, especially for 2 h calcination duration. For this reason, morphology studies using SEM were concentrated on the barium hexaferrite ceramics calcined at 900 °C for 2 h.

For the morphology of the barium hexaferrite platelets, in the case of the synthesis at 900 °C in NaCl flux, corners of the platelets became rounder (Fig. 2(e)). This is speculated to be caused by the selective desorption from the corners as a result of chemical potential change around the sharp corners of the platelets in the molten NaCl flux. In the case of platelet synthesis in KCl flux, either no desorption occurred or desorption occurred homogenously on all the surfaces and corners of the platelets so that platelet shape with sharp corners was preserved (Fig. 2(a)).

The aspect ratios of the platelets were approximately 3 to 4 for all calcination conditions. In addition to the platelet size and morphology, yield (mass of products/mass of raw materials) and amount of barium hexaferrite formation in the structure are crucial. Since the amount of flux evaporation during calcinations is unknown, yield of the barium hexaferrite ceramic production was calculated by ignoring the flux as raw material and product. A typical batch of 1.32 g containing equal amounts of salt and oxide/carbonate gives 0.53 g barium hexaferriteresulting in the yield of 80%. Furthermore, Fig. 3 shows the amount of barium hexaferrite formed during calcination at 900 °C for 2 h as a function of flux composition which was determined using quantitative XRD analysis. It is obvious that formation of barium hexaferrite phase within the system was the lowest when synthesis was done in 100 wt% KCl flux. With the increase in the NaCl content, the amount of barium hexaferrite phase increased gradually up to 97.8% at 100 wt% NaCl flux composition.

Magnetization curves were taken at 300 K for the barium hexaferrite platelets synthesized at 900 °C for 2 h in 100 wt% KCl, 10 wt% NaCl, 44 wt% NaCl, 90 wt% NaCl and 100 wt%

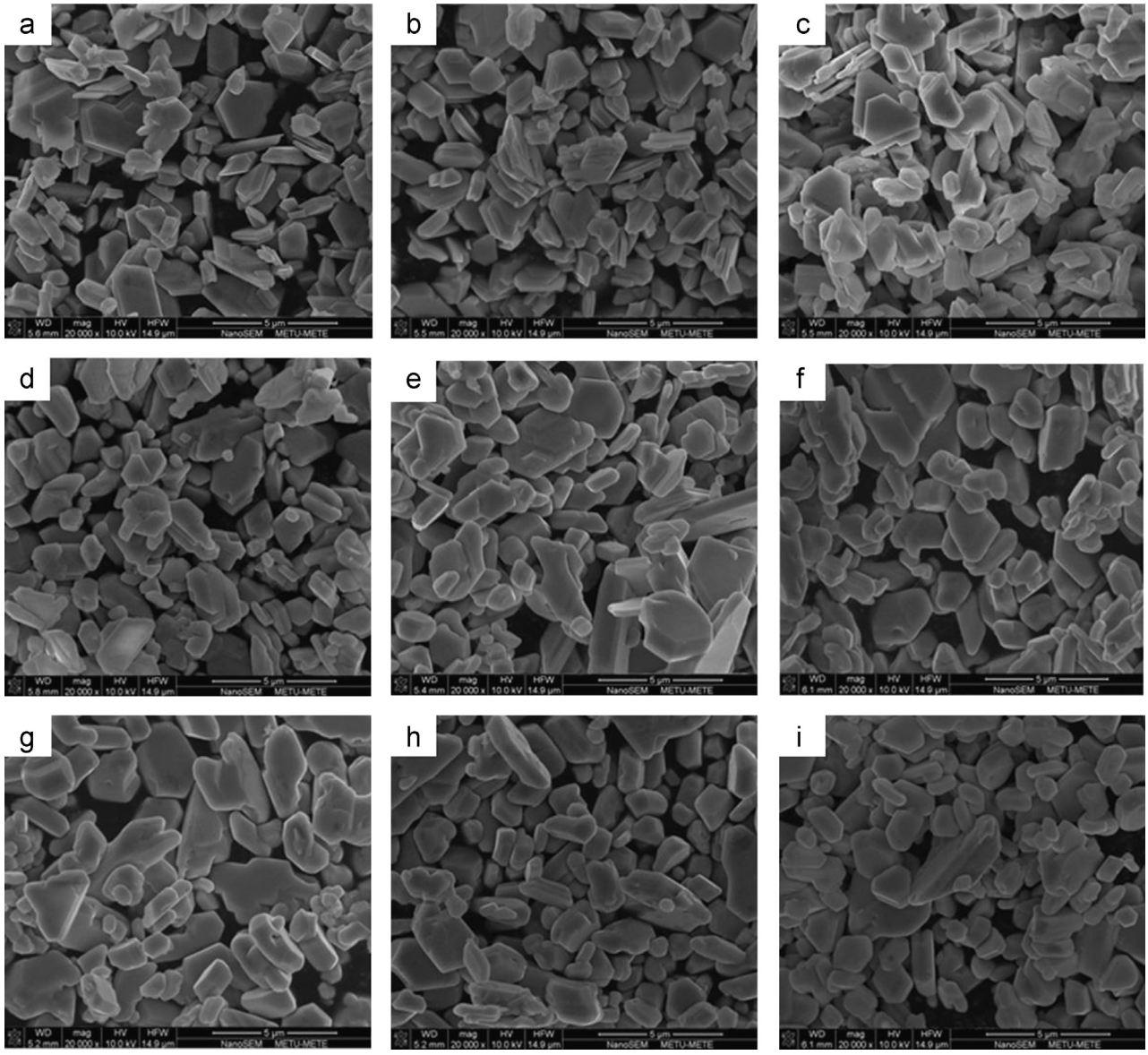

Fig. 2. SEM images of barium hexaferrite platelets calcined in (a) 100 wt% KCl, (b) 90 wt% KCl–10 wt% NaCl, (c) 80 wt% KCl–20 wt% NaCl, (d) 70 wt% KCl–30 wt% NaCl, (e) 44 wt% NaCl–56 wt% KCl (1:1 mol), (f) 70 wt% NaCl–30 wt% KCl, (g) 80 wt% NaCl–20 wt% KCl, (h) 90 wt% NaCl–10 wt% KCl, and (i) 100 wt% NaCl at 900 °C for 2 h.

NaCl. In Fig. 4, B–H curves of synthesized barium hexaferrite ceramics exhibit a clear hysteresis behavior for the magnetization under applied magnetic field. When the applied magnetic field is around 10 kO_e, the magnetization saturates.

As the NaCl content in the molten flux increases, the area under the hysteresis curve increases, and the ceramic reveals a stronger hard magnetic behavior (Fig. 4). The saturation magnetization (M_s), remanent magnetization (M_r), squareness ratio (M_r/M_s) and the coercive field (H_c) of the barium hexaferrite platelets obtained from Fig. 4 are given in Table 2. As the NaCl content increases, there is an increase in barium hexaferrite amount that improves the hard magnetic behavior of the ceramics. Although magnetic saturation values change around 55 emu/g for all flux compositions, the highest saturation value of 56.5 emu/g was obtained in the case of 44 wt% NaCl composition. On the other hand, the highest coercivity of 1600 O_e was obtained for 90 and 100 wt% NaCl flux compositions. It is clear that NaCl content increase in the flux improves the barium hexaferrite conversion which in turn results higher coercivity and remanent magnetization. High coercivity and remanent magnetization indicate the augmentation in the hard magnetic behavior of the synthesized ceramics.

4. Conclusions

Micron size barium hexaferrite ($BaFe_{12}O_{19}$) platelets were prepared by molten-salt synthesis method in various weight proportions of NaCl–KCl salt mixtures. It has been determined that Fe_2O_3 solubility in molten NaCl–KCl salts is negligible and barium hexaferrite forms by dissolution of BaO followed by diffusion of Ba^{+2} and O^{-2} ions in the flux. It was observed that NaCl plays a prominent role on the formation of barium

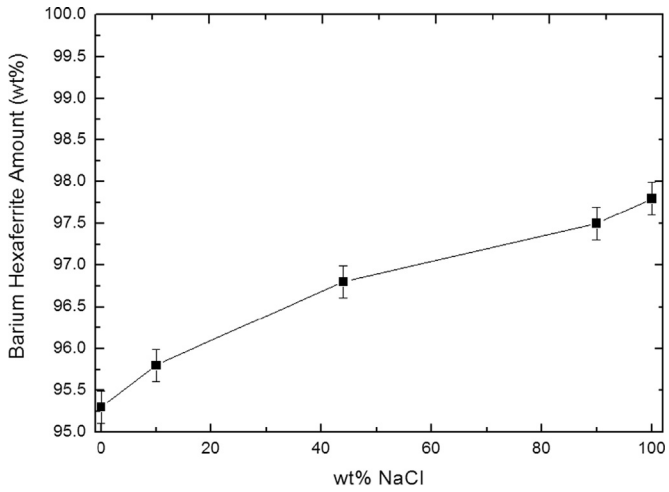

Fig. 3. Quantitative XRD analysis of platelets calcined at 900 °C for 2 h in varying flux compositions.

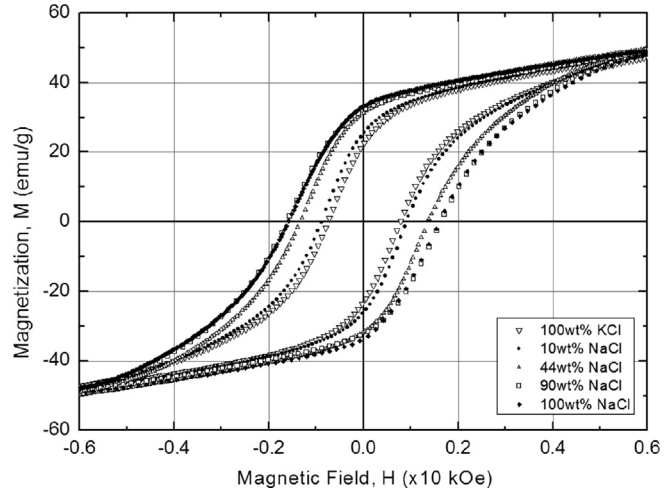

Fig. 4. 300 K hysteresis curves of barium hexaferrite ceramics synthesized in 100 wt% KCl, 10 wt% NaCl, 44 wt% NaCl, 90 wt% NaCl and 100 wt% NaCl.

hexaferrite phase. As the content of NaCl increases, barium hexaferrite formation is enhanced. The highest conversion which is 97.8% is obtained in the case of 100 wt% NaCln flux. The morphology of the barium hexaferrite platelets are also influenced by the NaCl–KCl flux composition. Platelets synthesized in NaCl flux are rounded which can be attributed to the directional desorption of barium hexaferrite in NaCl rich fluxes. However, either no desorption or homogenous desorption on all the platelet surfaces occurs in the case of KCl leading to the preservation of cornered platelet shape. The platelets synthesized in NaCl have higher average sizes than those in KCl.

Flux composition has clear impact on the magnetic properties of barium hexaferrite ceramics mainly based on the efficiency of transformation. Increasing NaCl content in the flux improves the coercivity and remanent magnetization of barium hexaferrite along with the area under the hysteresis curve leading to a more pronounced hard magnetic behavior in the synthesized ceramics. In conclusion, presented results

Table 2
Magnetic properties of barium hexaferrite ceramics synthesized in five different molten flux compositions.

Flux composition (wt%)	Barium hexaferrite amount(wt%)	H_c (Oe)	M_r (emu/g)	M_s (emu/g)	M_r/M_s
100KCl	95.3	753	21.9	55.0	0.40
10NaCl	95.8	838	25.0	54.3	0.45
44NaCl	96.8	1380	31.4	56.5	0.55
90NaCl	97.5	1600	32.0	55.2	0.58
100NaCl	97.8	1600	33.2	55.6	0.59

demonstrate that the composition of the NaCl–KCl flux as the synthesis medium plays an important role on the extent of barium hexaferrite formation, resulting platelet morphology and the magnetic properties.

Acknowledgments

We would like to thank Assist. Prof. Dr. Y. Eren KALAY (Middle East Technical University, Department of Metallurgical and Materials Engineering) for his help and guidance in the XRD quantitative analysis part of the article.

References

[1] H.I. Hsiang, Effects of glass addition on magnetic properties of $3Ba_{0.5}Sr_{0.5}O_2CoO_{12}Fe_2O_3$ for multilayer chip inductors, Part 1: Regular Papers and Short Notes and Review Papers, Japanese Journal of Applied Physics 41 (8) (2002) 5137–5141.

[2] H.I. Hsiang, C.S. Hsi, T.C. Lee, C.H. Chang, Effects of glass additions on $3Ba_{0.5}Sr_{0.5}O_2CoO_{12}Fe_2O_3$ for high-frequency applications, Journal of Magnetism and Magnetic Materials 268 (1–2) (2004) 186–193.

[3] R.M. Almeida, W. Paraguassu, D.S. Pires, R.R. Corrêa, C.W. de Araujo Paschoal, Impedance spectroscopy analysis of $BaFe_{12}O_{19}$ M-type hexaferrite obtained by ceramic method, Ceramics International 35 (6) (2009) 2443–2447.

[4] Y. Liu, M.G.B. Drew, J. Wang, M. Zhang, Preparation, characterization and magnetic properties of the doped barium hexaferrites $BaFe_{12-2x}Co_{x/2}Zn_{x/2}Sn_xO_{19}$, $x=0.0-2.0$, Journal of Magnetism and Magnetic Materials 322 (7) (2010) 814–818.

[5] M.C. Dimri, S.C. Kashyap, D.C. Dube, Electrical and magnetic properties of barium hexaferrite nanoparticles prepared by citrate precursor method, Ceramics International 30 (7) (2004) 1623–1626.

[6] W. Roos, Formation of chemically coprecipitated barium ferrite, Journal of the American Ceramic Society 63 (11–12) (1980) 601–603.

[7] D. Barb, L. Diamandescu, A. Rusi, D. TĂrĂbĂsanu-MihĂilĂ, M. Morariu, V. Teodorescu, Preparation of barium hexaferrite by a hydrothermal method: structure and magnetic properties, Journal of Materials Science 21 (4) (1986) 1118–1122.

[8] S. Singhal, T. Namgyal, J. Singh, K. Chandra, S. Bansal, A comparative study on the magnetic properties of $MFe_{12}O_{19}$ and $MAlFe_{11}O_{19}$ (M=Sr, Ba and Pb) hexaferrites with different morphologies, Ceramics International 37 (6) (2011) 1833–1837.

[9] Y. Du, H. Gao, X. Liu, J. Wang, P. Xu, X. Han, Solvent-free synthesis of hexagonal barium ferrite ($BaFe_{12}O_{19}$) particles, Journal of Materials Science 45 (9) (2010) 2442–2448.

[10] E.K. Akdogan, R.E. Brennan, M. Allahverdi, A. Safari, Effects of molten salt synthesis (MSS) parameters on the morphology of $Sr_3Ti_2O_7$ and $SrTiO_3$ seed crystals, Journal of Electroceramics 16 (2) (2006) 159–165.

[11] R.H. Arendt, J.H. Rosolowski, J.W. Szymaszek, Lead zirconate titanate ceramics from molten salt solvent synthesized powders, Materials Research Bulletin 14 (5) (1979) 703–709.

[12] J.P. Wang, Y. Liu, M. Hu, M.L. Zhang, Effects of different molten-salt on the synthesis of hexagonal barium ferrite, Chinese Journal of Aeronautics 19 (2006) S206–S209 (Suppl.).
[13] S. Dursun, R. Topkaya, N. Akdoan, S. Alkoy, Comparison of the structural and magnetic properties of submicron barium hexaferrite powders prepared by molten salt and solid state calcination routes, Ceramics International 38 (5) (2012) 3801–3806.
[14] R.H. Arendt, The molten salt synthesis of single magnetic domain $BaFe_{12}O_{19}$ and $SrFe_{12}O_{19}$ crystals, Journal of Solid State Chemistry 8 (4) (1973) 339–347.
[15] C. Duran, G.L. Messing, S. Trolier-McKinstry, Molten salt synthesis of anisometric particles in the SrO–Nb_2O_5–BaO system, Materials Research Bulletin 39 (11) (2004) 1679–1689.
[16] Y.T. Chien, H.C. Pan, Y.C. Ko, Preparation and properties of barium ferrite using hot-rolled mill scale, Journal of the American Ceramic Society 72 (8) (1989) 1328–1332.
[17] D.B. Hovis, K.T. Faber, Textured microstructures in barium hexaferrite by magnetic field assisted gelcasting and templated grain growth, Scripta Materialia 44 (11) (2001) 2525–2529.
[18] S. Alkoy, C. Duran, D.A. Hall, Electrical properties of textured potassium strontium niobate ($KSr_2Nb_5O_{15}$) ceramics fabricated by reactive templated grain growth, Journal of the American Ceramic Society 91 (5) (2008) 1597–1602.
[19] R.H. Arendt, Liquid-phase sintering of magnetically isotropic and anisotropic compacts of $BaFe_{12}O_{19}$ and $SrFe_{12}O_{19}$, Journal of Applied Physics 44 (7) (1973) 3300–3305.